RSC Advances

PAPER

View Article Online
View Journal | View Issue

Cite this: *RSC Adv.*, 2017, **7**, 25811

Selective removal Pb(II) ions form wastewater using Pb(II) ion-imprinted polymers with bi-component polymer brushes†

Xubiao Luo,[a] Haiyan Yu,[a] Yu Xi,[a] Lili Fang,[a] Lingling Liu[a] and Jinming Luo*[b]

Ion imprinted polymers (IIPs) are very difficult to apply in actual wastewater containing solid particles and floccules due to the imprinting hole blockage of losing adsorption performance. Pb(II) ion-imprinted polymers with bi-component polymer brushes (grafted-IIP) are synthesized and its anti-interference performance was studied. The maximum adsorption capacity of ungrafted Pb(II) ion-imprinted polymers (RAFT-IIP) and grafted-IIP was 53.8 mg g^{-1} and 38.5 mg g^{-1}, respectively. Introduction of bi-component polymer brushes did not change significantly adsorption selective performance of grafted-IIP and adsorption rate for Pb(II) ion. Moreover, grafted-IIP possesses satisfactory anti-interference and anti-clogging ability for flocculation and solid particles. Grafted-IIP could retain more than 80.5% adsorption capacity of the maximum adsorption capacity in the process of treating Dexing copper mine wastewater, and can be repeated at least six times. In addition, XPS revealed that Pb(II) ion adsorption mainly depended on S site of imprinted cavities, and forms four coordination bonds with S–C and S=C of 3-allylrhodanine, and bi-component brushes played an indispensable role for anti-interference ability by Al–O coordination bond, hydrogen bond, or hydrophobic interactions. The ion-imprinted polymers with bi-component polymer brushes have good application prospects for the treatment of the complicated wastewater.

Received 27th March 2017
Accepted 1st May 2017

DOI: 10.1039/c7ra03536e

rsc.li/rsc-advances

1. Introduction

Heavy metals as a representative contaminant extensively exist in water, which are poisonous to human health because they can accumulate in living tissues and food chain.[1,2] The removal of heavy metal and organic pollutant in wastewater treatment process become a remarkable concern issue.[3–11] Lead (Pb(II)) is one of the toxic metals enumerated among the priority heavy metals pollutants,[12,13] and various sorbents were used to remove Pb(II) ions from wastewater in recent study, for instance, tea waste,[14–16] natural biosorbent,[16–18] bentonite,[19–21] magnetic nano-particles,[22,23] activated carbon,[24,25] metal–organic frameworks,[26,27] mesoporous silica materials.[28] However, most of the adsorption technology are essentially a transfer of pollutants, which bears tremendous secondary pollution risk. Ion imprinted polymers are hope to resolve above problem of secondary pollution due to its high recognition and selectivity. Our research group carried out a lot of works about ion imprinted adsorbents and dedicated to develop a new practical recycling product technology.[29–32] Other research group took the sol–gel method to prepare the Pb(II)-IIP, using dual functional monomers, that have highly selective for Pb(II),[33] reverse emulsion polymerization prepare Pb(II)-surface imprinted polymers and successfully used in actual water samples,[30] and magnetic porous nanoparticles Pb(II)-imprinted polymer to selective separate and detect Pb(II) in the food sample.[34] However, imprinted cavities were easily blocked by solid particles and complexes flocculent in actual wastewater, thus limiting its wide range of applications. Thus, developing an ion imprinted polymer with anti-interference ability is very important for wastewater applications.

In order to solve above problem, our research group designed lithium ion imprinted polymers with hydrophilic PHEMA polymer brushes and investigated the role of grafting density on anti-interference and anti-blockage in wastewater.[35] Furthermore, PHEMA brushes possess well hydrophilic,[36,37] but we also found hydrophilic PHEMA brushes could effectively adhere fine particles and flocculants though van der Waals force interactions and displayed good anti-interference ability. In order to further increase anti-clogging ability, we modified bi-component polymer brushes on the surface cadmium ion polymer and verified appropriate rigid component (PS) introduction on bi-component brushes could enhance ion imprinted

[a]*Key Laboratory of Jiangxi Province for Persistent Pollutants Control and Resources Recycle, Nanchang Hangkong University, Nanchang 330063, P.R. China. E-mail: luoxubiao@126.com; Fax: +86 791 395373; Tel: +86 791 3953372*

[b]*School of Civil and Environmental Engineering and Brook Byers Institute for Sustainable Systems, Georgia Institute of Technology, Atlanta, 30332, USA. E-mail: bradyluo@126.com*

† Electronic supplementary information (ESI) available. See DOI: 10.1039/c7ra03536e

polymer anti-clogging ability. Moreover, we firstly provided the concept of the "broom effect".[38] However, it has not been applied widely to other heavy metal ion due to the differences of heavy metal ions chemical properties in wastewater.

For the sake of applying to other heavy metal ions and investigating further bi-component bush anti-interference performance, we have designed Pb(II) ion-IIP with the surface modification of bi-component polymer brushes included polymer hydroxyethyl methacrylate (PHEMA) and polymer styrene (PS) *via* reversible addition–fragmentation chain transfer polymerization (RAFTPP). The bi-component anti-interference performance were investigated through a series of simulated wastewater containing solid particles, floccules and the actual factory wastewater. We used XPS to reveal the mechanism of anti-interference ability. And we verified ion imprinted polymer with bi-component polymer brushes had a high potential in the practical wastewater. The next step of work need to discuss the effect of chain lengths of polymer brushes on the anti-interference ability in order to make it the most of anti-interference performance.

2. Experimental

2.1 Materials and chemicals

All the detailed of the materials and chemicals are provided in the ESI.†

2.2 Apparatus

All the primary used apparatus are shown in the ESI.†

2.3 Synthesis of RAFT-IIP/NIP and grafted-IIP/NIP microspheres by RAFTPP

The detailed procedure of synthesis imprinted materials is described in the ESI.†[39]

2.4 Batch adsorption experiments

All the adsorption experiments were conducted according to the following steps. First of all, 20 mg adsorbents were added into 20 mL adsorbate solution, then shook from 4 h in incubator shaker (Jingqi, IS-RDD3, USA) at 25 °C. After the adsorption equilibrium, the remaining of Pb(II) concentrations (C_e) were measured by atomic absorption spectrum (AAS). The Pb(II) uptake capacity at equilibrium was calculated from equation:

$$q_e = \frac{(C_0 - C_e)V}{m} \quad (1)$$

where q_e represents the adsorption capacity (mg g^{-1}); C_0 and C_e are the initial and equilibrium concentrations of lead ions (mg L^{-1}), respectively; m is the mass of sorbents (g); and V is the volume of the metal ion solution (L).

pH is a significant impact on the adsorption to metal ions adsorption process. The adsorption effect of pH is evaluated though a series of pH gradient (3.0–6.0) control, 0.1 mol L^{-1} HCl and 0.1 mol L^{-1} NaOH were used for pH adjustment. In order to investigate the equilibrium adsorption of RAFT-IIP/NIP and grafted-IIP/NIP, an initial concentration of Pb(II) ranged from 100 to 600 mg L^{-1} was carried on isothermal adsorption experiment. Adsorption kinetic experiments were obtained by adding 250 mg of adsorbents into 250 mL of a 500 mg L^{-1} Pb(II) ion solution at room temperature, with constant stirring, samples were taken out at setting intervals time, then the adsorbents were separated by centrifugation.

2.5 Adsorption experiments in different media

Simulated wastewater containing solid particles and different kind of flocculants were applied to study the anti-interference ability of grafted-IIP. In this study, three kinds of particle sizes of SiO_2 (Fig. S1†) which included a wide range particle size distribution were synthesized to simulate solid particle distribution in real wastewater. SiO_2 particles were made into 1.0 mg mL^{-1} homogeneous solution in deionized water. In addition, three kinds of industrial-grade pure flocculants, universal exist in wastewater, including sodium carboxymethyl cellulose (CMC), poly aluminum chloride (PAC), and polyacrylamide (PAM) were also made into contain 1.0 mg mL^{-1} homogeneous floccules solution either single component or pairwise orthogonal flocculants. The concentration of Pb(II) ion in all aqueous samples was 500 mg L^{-1}.

In order to investigate the practical application ability of the RAFT-IIP and grafted-IIP, the real wastewater was used. The copper mine wastewater came from Dexing Copper Mine in Jiangxi, in which suspending white floccule and solid particle (Fig. S2†) with a series of other metal ions such as Cu(II), Zn(II), Co(II) and Ni(II) at pH of 2.30. In addition, we added $Pb(NO_3)_2$ into the real wastewater until the concentration of Pb(II) to 400 mg L^{-1} due to no Pb(II) ion.

3. Results and discussion

3.1 Character analysis

The morphologies and size distributions of the RAFT-IIP and grafted-IIP particles were characterized by SEM. As shown in Fig. 1, the RAFT-IIP and grafted-IIP polymers were both spherical particles with size distribution 300–830 nm and 700–1700 nm, respectively. From the insets in Fig. 1, surface of RAFT-IIP is more smooth than grafted-IIP, which verified polymer brushes were grafted successfully on surface of imprinted microspheres. The FT-IR spectra (Fig. 2(a)) was employed to characterize RAFT-IIP and grafted-IIP. The spectrum peak at approximately 3440 cm^{-1} due to –OH stretching from PHEMA was observed in the spectra of the grafted-IIP/NIP, while the RAFT-IIP/NIP FTIR spectrum were not observed. Characteristic peaks corresponding to the C=S stretching at approximately 1043 cm^{-1} confirms the existence of dithioester groups and the C=O vibration at 1725 cm^{-1} from the bonded PHEMA was seen clearly.[40] Additionally, the PS polymer brushes FT-IR absorption characteristic peaks were overlapped with in the spectra of CDB characteristic peaks at approximately 2995 cm^{-1}, 2955 cm^{-1}, 750–1400 cm^{-1} indicate aliphatic C–H stretching, aromatic C–H stretching 3043 cm^{-1}, 1500 cm^{-1} and 700–1400 cm^{-1} denote aliphatic C–H stretching, aromatic C–H stretching.[41,42] The signal at

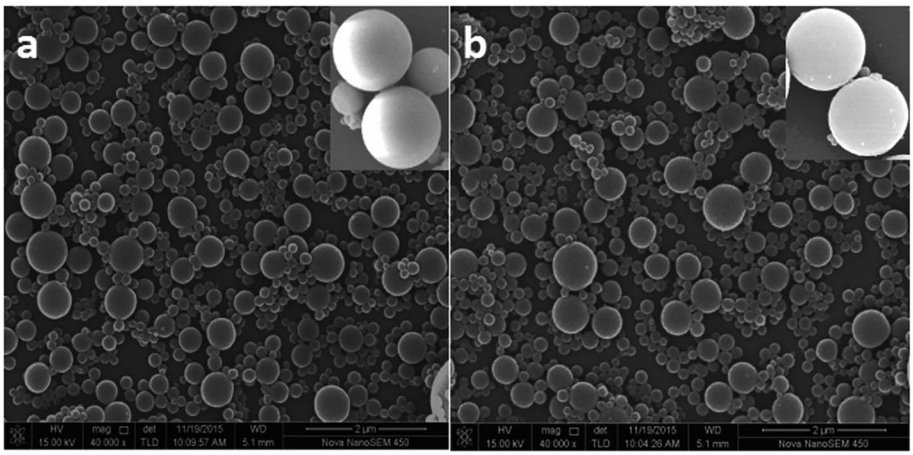

Fig. 1 SEM images of the RAFT-IIP (a) and grafted-IIP (b) microspheres.

3440 cm^{-1} is ascribed to –OH stretching from PHEMA, however, the peak is not observed in FTIR of RAFT-IIP/NIP spectrum (Fig. 2(a)). This another evidence revealed grafted-IIP had been prepared successfully. In addition, in comparison with RAFT-IIP, the isoelectric point of grafted-IIP shifted toward the left to 0.18 unit (Fig. 2(b)). It was possibly that the function groups of PHEMA and PS brushes have an impact on charge distribution on the surface of grafted-IIP, thus, resulting in the change of the zeta potential. This results further demonstrated that hydrophilic PHEMA and PS polymer brushes have successfully grafted on the RAFT-IIP/NIP microspheres surface by RAFT precipitate polymerization.

The thermal stability of the RAFT-IIP and grafted-IIP were investigated *via* thermogravimetry at the temperature from 50 °C to 700 °C. The results in Fig. 2(c) show the change trend of RAFT-IIP and grafted-IIP is the same, and the decompose temperature is both above 250 °C. Introduction of bi-component bushes did almost not change the thermal stability performance and only reduce the loss weight ratio at the same temperature. By eqn (2) (in the ESI†) calculation obtained the grafting ratios are 0.72 and 1.1 for grafted-IIP and grafted-NIP, respectively. GPC analysis demonstrated molecular weights and PDI of grafted-IIP and grafted-NIP are 1.01 and 1.02 (Table S1†), respectively. These results verify the imprinted polymer surface is successfully

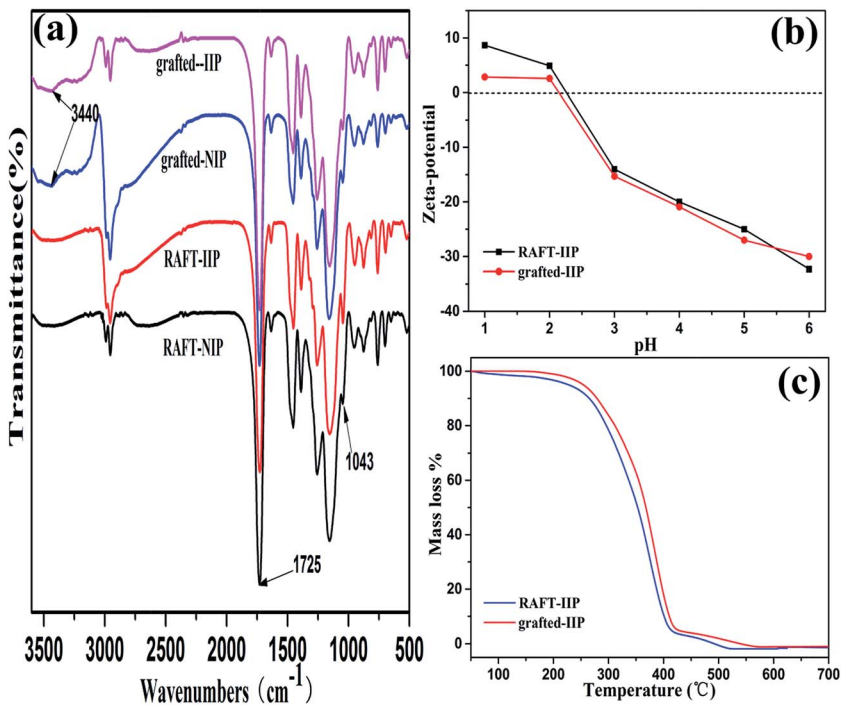

Fig. 2 FT-IR spectra of the RAFT-IIP/NIP and grafted-IIP (a) and zeta-potential of RAFT-IIP and grafted-IIP (b), thermogravimetric curves of the RAFT-IIP and grafted-IIP (c).

grafted with bi-component polymer brushes and graft density and chain length maybe have greatly influenced on anti-interference ability of imprinting adsorbents.

3.2 Effect of pH on Pb(II) ion adsorption

As is well known that there is a significant impact on the adsorption solution of pH for metal ions adsorption process. Under alkaline conditions (pH $\geq$ 7.0), Pb(II) ions are in precipitation state, it is not appropriate for ion imprinting to explore application. Thus, the Pb(II) solutions with various pH (3–6) were systematically investigated. As seen from the Fig. 3, adsorption capacity of RAFT-IIP/NIP increases sharply at pH value ranging from 3.0 to 4.0, then decreases at pH > 4.0, the largest adsorption amounts were 47.0 mg g^{-1} and 18.0 mg g^{-1}, respectively. Nevertheless grafted-IIP/NIP increases quickly at pH ranging from 3.0 to 5.0, decreases at pH > 5.0 afterward, which have 29.5 mg g^{-1} and 15.0 mg g^{-1}, respectively. The optimum pH value of RAFT-IIP/NIP and grafted-IIP/NIP are 4.0 and 5.0, respectively. Meanwhile, the zeta-potential of RAFT-IIP and grafted-IIP are −20 and −27 mV, respectively (Fig. 2(b)). Negative surface of RAFT-IIP and grafted-IIP is more benefited for adsorption of positively charged Pb(II) ion.

3.3 Adsorption capacity in different water

In order to investigate anti-interference of RAFT-IIP/NIP and grafted-IIP/NIP, their isothermal equilibrium adsorption was studied in pure water and simulation wastewater. Fig. 4 presents that adsorption experiment data in pure water are fitted by the Langmuir and Freundlich nonlinear isotherms models. The parameters of the isotherm model are summarized in Table 1. These results demonstrated Pb(II) ion adsorption was monolayer adsorption on the surface RAFT-IIP/NIP and grafted-IIP/NIP due to better fitness Langmuir model. Furthermore, the calculated values of q_e indicates that RAFT-IIP/NIP and grafted-IIP/NIP have the potential of remove Pb(II) ion from aqueous solutions with the saturated adsorbed capacity to 71.6 mg g^{-1}, 36.4 mg g^{-1} and 59.6 mg g^{-1}, 26.2 mg g^{-1}, respectively. It can be seen clearly that RAFT-IIP/NIP could adsorb more Pb(II) ion than grafted-IIP/NIP. That is because bi-component brushes without adsorption site resulted in decrease of imprinted cavities unit mass.

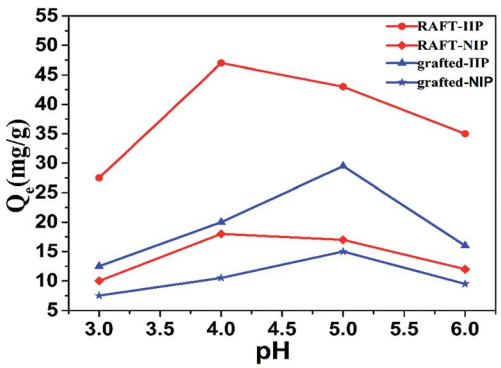

Fig. 3 Effect of pH on adsorption capacity of RAFT-IIP/NIP and grafted -IIP/NIP. Pb(II) initial concentration 400 mg L^{-1}; adsorption time 12 h.

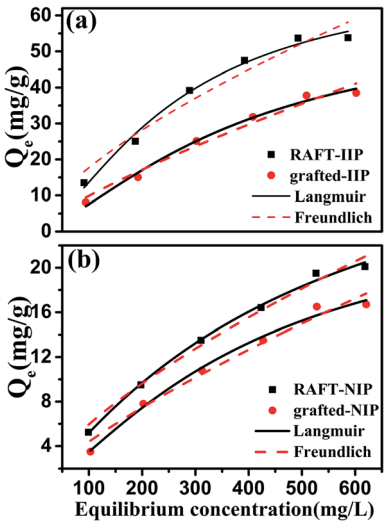

Fig. 4 Langmuir and Freundlich adsorption isotherm of RAFT-IIP/NIP and grafted-IIP/NIP.

Fig. 5 showed Pb(II) ion adsorption capacities of RAFT-IIP/NIP and grafted-IIP/NIP in different simulated wastewater containing SO_2 and flocculants. Firstly, grafted-IIP/NIP adsorption capacities in any simulated wastewater are all higher than RAFT-IIP/NIP. This results verified that introduction of bi-component brushes on the surface of IIP is very important for enhancing anti-interference ability of IIP. Secondly, Pb(II) ion adsorption capacities on grafted-IIP decreased gradually with decrease of particle size of SO_2 in simulated wastewater. It might be because bi-component polymer brushes could prevent large size particle entering into imprinted cavity. However, smaller size particle could reach the surface of imprinted microsphere through the space between the polymer brushes and blocked partially imprinted cavity. The size of solid particles was in the range of 185–300 nm in Dexing Copper Mine wastewater (Fig. S2†). Grafted-IIP show the best anti-clogging ability for greater than 100 nm particles, this further explained bi-component polymer brushes are suitable for anti-blocking in treating Dexing Copper Mine wastewater. Thirdly, grafted-IIP has also good anti-interference for flocculation in simulated wastewater. With increase of flocculation concentration, the adsorption capacities decreased gradually. The order of anti-interference is PAC > PAM > CMC. This results can be explained by interaction force between flocculation and PHEMA in bi-component. PAC coordination force with PHEMA is bigger than PAM hydrogen bonding force with PHEMA, bigger than CMC hydrogen bonding force with PHEMA. Above results full proved bi-component polymer brushes grafted on the imprinting surface has good anti-interference ability in containing SiO_2 solid particles and flocculation particles water solution.

3.4 Adsorption kinetics

Adsorption rate is an important factor for removal Pb(II) ion from wastewater. For sake of investigating effect before and

Table 1 Parameters of the Langmuir and Freundlich isotherm for Pb(II) adsorption

	Freundlich isotherm parameters			Langmuir isotherm parameters		
T	n	K_F (mg g^{-1})	R^2	Q_m (mg g^{-1})	b (L mg^{-1})	R^2
RAFT-IIP	1.49	0.80	0.95	71.56	0.125×10^{-3}	0.98
RAFT-NIP	1.45	0.25	0.98	36.35	0.941×10^{-3}	0.99
Grafted-IIP	1.26	0.25	0.97	59.61	0.174×10^{-3}	0.99
Grafted-NIP	1.31	0.13	0.97	26.24	0.279×10^{-3}	0.99

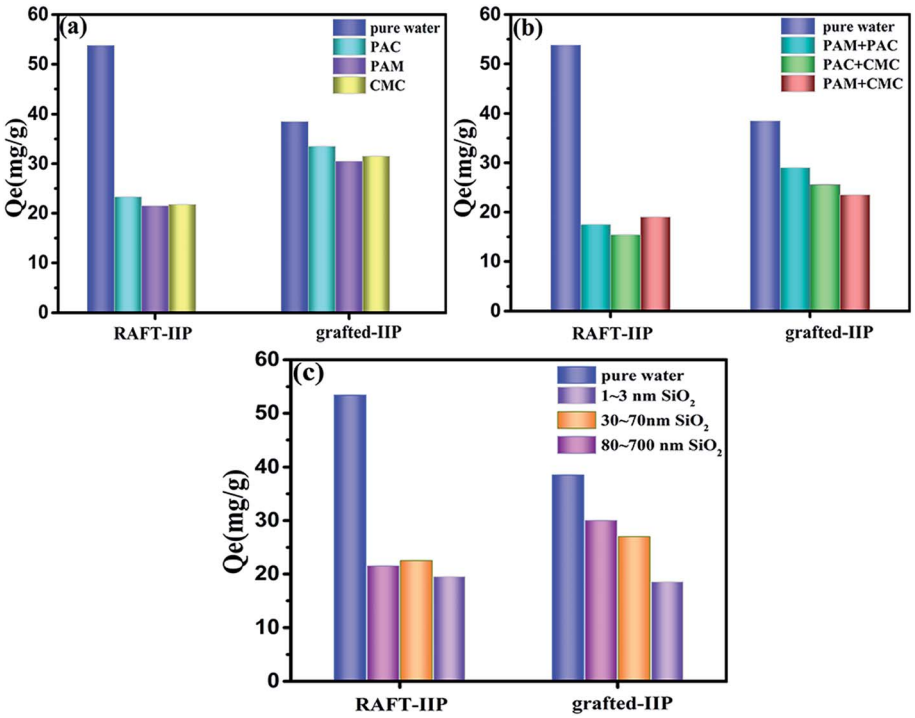

Fig. 5 Adsorption experiments of RAFT-IIP and grafted-IIP in simulated wastewater; in a single component flocculant (a); in the mixed component flocculant (b); in the solid particles SiO_2 (c).

after grafted bushes, adsorption kinetics of RAFT-IIP/NIP and grafted-IIP/NIP were studied. Fig. 6 showed Pb(II) ion bounded amounts on RAFT-IIP/NIP and grafted-IIP/NIP increased sharply in initial 10 min, then increased slowly, and finally attained its saturation value after 36 min and 60 min, respectively. The kinetic data of RAFT-IIP/NIP and grafted-IIP/NIP were fitted using the pseudo-first-order (eqn (8) in the ESI†) and the pseudo-second-order (eqn (9) in the ESI†) models. From the comparison between the experimental adsorption capacity (q_{exp}) and calculated adsorption capacity (q_{cal}), it shows that q_{exp} are very close to q_{cal} values for the pseudo-second-order kinetics (Table 2). Moreover, the pseudo-second-order model correlation coefficient values are higher than that of pseudo-first-order model. This result demonstrated the pseudo-second-order models is more suitable than pseudo-first-order model. Thus, RAFT-IIP/NIP and grafted-IIP/NIP for Pb(II) ion adsorption belongs to the chemical adsorption. In addition, the kinetic rate constant (k) of RAFT-IIP is about 2 times than grafted-IIP. This results can be explained that introduction of bi-component

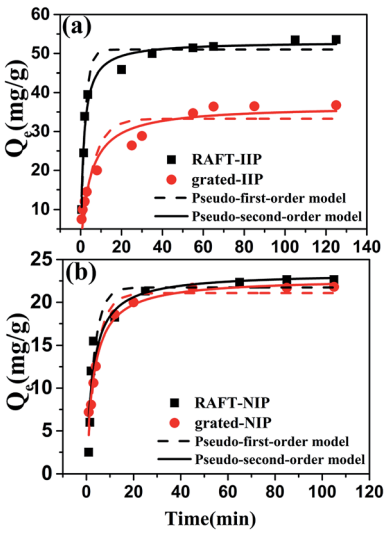

Fig. 6 Adsorption kinetics for Pb(II) ion adsorption for RAFT-IIP/NIP and grafted-IIP/NIP fitted with pseudo-first and pseudo-second order models.

Table 2 Parameters of the pseudo-first-order and pseudo-second-order for Pb(II) adsorption

		Pseudo-first-order			Pseudo-second-order			
Metals	q_e, exp (mg g^{-1})	k_1 (L min^{-1})	q_e, cal (mg g^{-1})	R^2	k_2 (g (mg min)$^{-1}$)	q_e, cal (mg g^{-1})	h_0 (mg (g min)$^{-1}$)	R^2
RAFT-IIP	53.6	0.47	50.99	0.97	0.0126	53.02	35.42	0.97
RAFT-NIP	22.65	0.31	21.73	0.91	0.0154	23.45	8.468	0.91
Grafted-IIP	36.75	0.17	33.28	0.86	0.0057	36.61	7.6396	0.94
Grafted-NIP	21.80	0.24	21.07	0.96	0.0141	22.79	7.3233	0.98

bushes increased mass transfer resistance of Pb(II) ion. However, this is difference with one-component hydrophilic PHEMA brushes. Perhaps intertwined partially benzene ring in bi-component bushes blocking Pb(II) ion movement, however, only one-component hydrophilic PHEMA bushes did not exist in intertwining and stretched out adequately in aqueous solutions, then, did not hinder mass transfer of Pb(II) ion. In summary, introduction of bi-component bushes on surface of IIP would reduce mass transfer rate, but 1 h balance time could be accepted in practical application.

3.5 Adsorption selectivity study

To confirm whether grafted polymer brushes have an effect on the selectivity of IIP, Cr(II), Zn(II), Co(II) and Ni(II) with same charge and similar size were used as competitive ion. Fig. 7 described RAFT-IIP/NIP and graft-IIP/NIP exhibits obvious higher Pb(II) ion uptake capacities than other Cr(II), Zn(II), Co(II) and Ni(II) ions. The selectivity coefficient and relative selectivity coefficients were calculated and listed in Table 3. The selectivity coefficient and relative selectivity coefficients of RAFT-IIP are bigger than grafted-IIP, which demonstrated bi-component brushes have an influence on the selectivity of IIP. Perhaps rigid styrene changed IIP hydrophilic properties and reduced distribution ability of metal ion. However, from the viewpoint of all relative selectivity factor $\beta > 1.2$, grafted-IIP still retained good selective performance for Pb(II) ion.

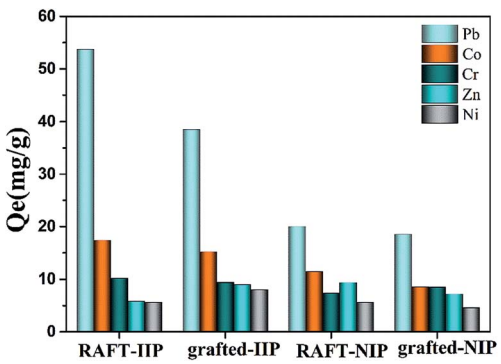

Fig. 7 The selectivity of RAFT-IIP/NIP and grafted-IIP/NIP. The initial Pb(II), Cr(II), Zn(II), Co(II) and Ni(II) ions concentration was 500 mg L^{-1}.

3.6 Anti-interference and adsorption mechanism analysis

In order to investigate the anti-interference mechanism, XPS was used to analyze interaction between bio-component polymer brushes and PAC on surface of grafted-IIP. We selected PAC as observed object from three flocculation because there are not Al element in grafted-IIP and the change after and before adsorption is easy to be analyzed. The typical new peaks of Al (Al 2s, Al 2p) appeared in the wide-scan XPS spectra in Fig. 8(a), which demonstrated the PAC adhered to the surfaces of grafted-IIP. In addition, Fig. 8(b) shows the O 1s spectra of RAFT-IIP and grafted-IIP after adsorption. There is a new peak appear at 531.6 eV binding energy, indicating that O atoms is combined with PAC. Furthermore, the C–O peaks shifted to lower binding energy, which verified O atoms share electrons with Al resulted in the decrease of electron densities of O atoms. The new Al–O coordination and decrease of O atoms electron densities confirmed the anti-interference ability of bi-component bushes mainly depends on Al–O coordination bond.[43,44]

The adsorption mechanism was also investigated by XPS. The signals of Pb 4f and S 2p were observed after adsorption in Fig. 9(a). Furthermore, in Fig. 9(b) the peaks at 164.75 and 162.97 eV corresponded to S–C bonds ($S_{3/2p}$ and $S_{1/2p}$)[45] were shifted toward lower binding energy to 163.48 eV and 162.12 eV after adsorption of Pb ion from wastewater. In addition, the peaks at approximately 163.57 and 161.79 eV corresponded to S=C bond ($S_{3/2p}$ and $S_{1/2p}$) were shifted toward lower values to 163.48 and 160.94 eV after adsorption,

Table 3 Selectivity Parameters of RAFT-IIP/NIP and grafted-IIP/NIP for Pb(II) adsorption

	RAFT-IIP		RAFT-NIP			Grafted-IIP		Grafted-NIP		
Metal ions	K_D	α	β	K_D	α	D	α	β	K_D	α
Pb(II)	115.04			39.96		79.88			36.85	
Zn(II)	11.31	10.17	4.70	18.45	2.17	17.65	4.52	1.73	14.07	2.62
Ni(II)	9.81	11.73	2.88	9.81	4.07	14.07	5.68	1.24	8.04	4.58
Co(II)	34.04	3.38	1.86	22.04	1.81	29.61	2.70	1.21	16.54	2.23
Cr(II)	18.19	6.32	2.08	13.13	3.04	16.74	4.77	1.96	15.11	2.44

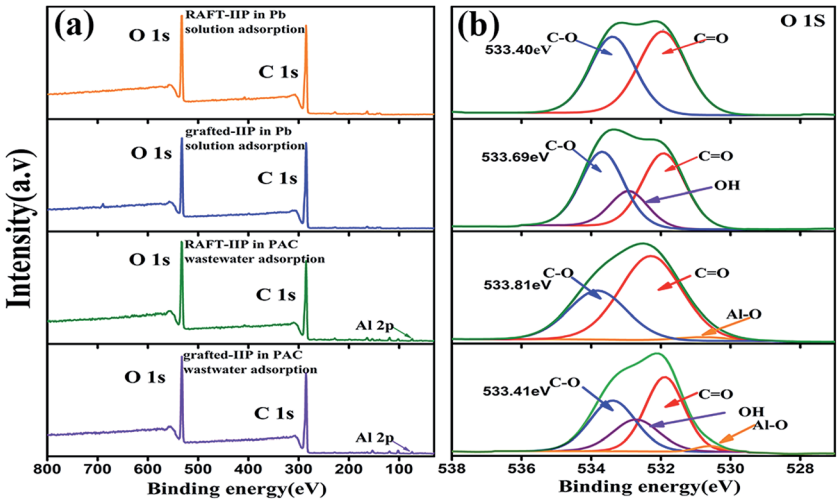

Fig. 8 XPS wide scan spectrum (a) and O 1s spectrum before and after adsorption in PAC wastewater for the RAFT-IIP and grafted-IIP (b).

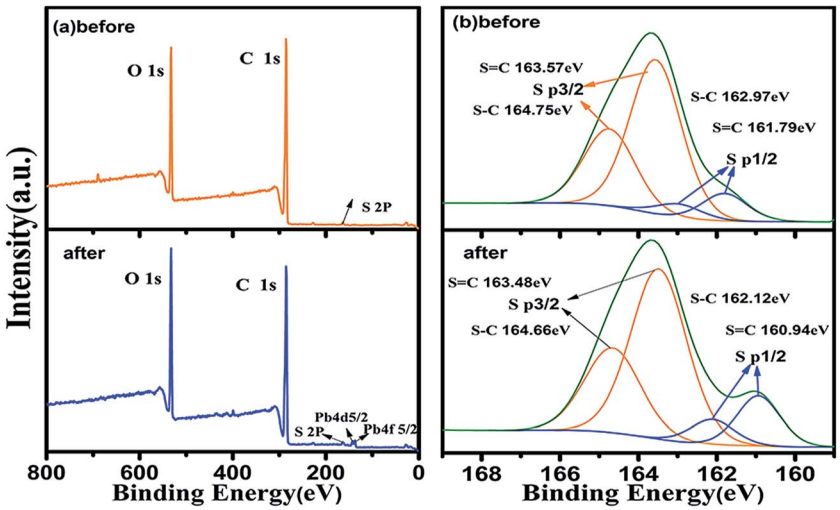

Fig. 9 XPS characterization of RAFT-IIP before and after Pb(II) adsorption. (a) XPS survey spectra along with the spectra of C 1s, O 1s, Pb 4d 4f ; (b) the high-resolution XPS spectra of S 2p before and after Pb(II) adsorption.

respectively. These results revealed S–C and S=C of functional monomer 3-allylrhodanine are binding site of Pb ion. In general, Pb coordination structure are composed of Pb ion and four organic ligands. On this basis, we can conclude that Pb ion forms coordination bonds with two 3-allylrhodanine functional monomer. This finding indicates that the S site of imprinted cavities has played an indispensable role for Pb(II) ion selective adsorption.

3.7 Application to actual wastewater and reusability

In order to investigate thoroughly the anti-interference of the bi-component polymer brushes, RAFT-IIP/NIP and grafted-IIP/NIP were applied to treat Dexing Copper Mine wastewater. As shown in the Fig. 10, grafted-IIP can retain more than 80.5% adsorption capacity for Dexing Copper Mine wastewater. However, RAFT-IIP has only 25.7% of the original adsorption capacity.

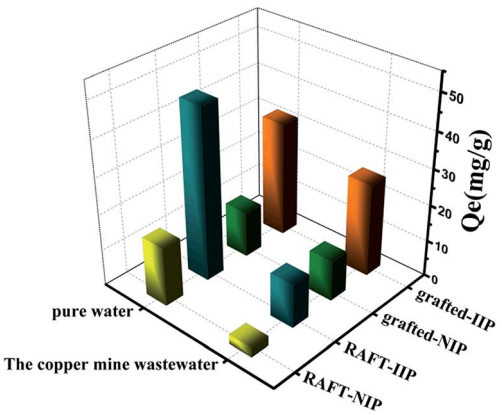

Fig. 10 Adsorption experiments with the RAFT-IIP/NIP and grafted -IIP/NIP in real wastewater.

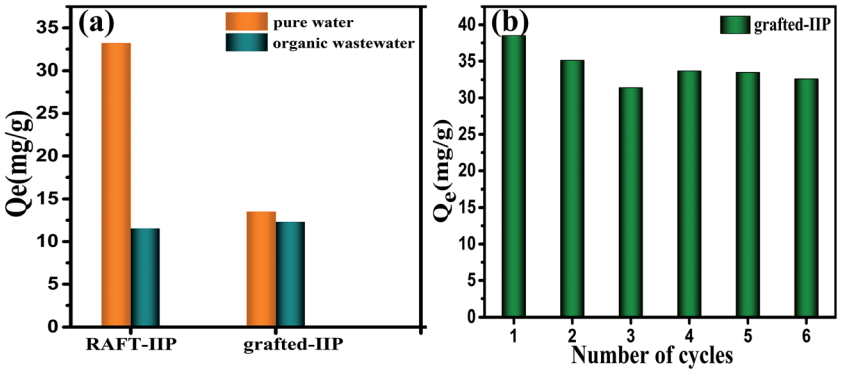

Fig. 11 Adsorption experiments with the RAFT-IIP and grafted-IIP pharmaceutical wastewater (a) and Reusability of grafted-IIP (b).

These results showed the bi-component polymer brushes on the imprinting surface have excellent anti-interference ability for the actual complex wastewater.

In order to investigate organic pollutants effect on ion imprinted polymer adsorption performance in practical wastewater and the life of grafted-IIP, RAFT-IIP and grafted-IIP were applied to the pharmaceutical wastewater (the value of COD is 28 700 mg L^{-1}). As show in Fig. 11(a), grafted-IIP can retain more than 90.1% adsorption capacity in high content of organic matter. However, RAFT-IIP has only 34.7% of the original adsorption capacity. The result are agreement with in the practical wastewater and showed that high content of organic matter in wastewater have slight effect on the adsorption ability of ion imprinting polymer. The Pb(II) ion adsorption capacities of grafted-IIP did not almost decline after subsequent five adsorption–desorption cycles in Fig. 11(b), the image morphology of RAFT and grafted-IIP after five cycle is also no change (Fig. S3†). But it started to drop down 15.3% after the six cycle. Perhaps portion of grafted-IIP lost under the operation condition or a portion of the imprinted cavities were destroyed. These results show grafted-IIP has good regenerative ability and can be repeated use for long time.

4. Conclusions

In our work, we have successfully synthesized Pb(II)-IIP with bi-component polymer brushes and explored its anti-interference effect. For particle pollutants, grafted-IIP with bi-component brushes show the best anti-clogging ability for 100 nm particles, in comparison with 10 nm, and 40 nm particles. For flocculation pollutants, anti-interference ability order of grafted-IIP with bi-component brushes is PAC > PAM > CMC. Grafted-IIP could retain more than 80.5% adsorption capacity for Dexing Copper Mine wastewater, higher than 47.6% of RAFT-IIP. Introduction of bi-component brushes has not significant impact on the selectivity of IIP. The Pb(II) ion adsorption mainly depended on S site of imprinted cavities, and forms four coordination bonds with S–C and S=C of 3-allylrhodanine functional monomer. Bi-component brushes played an indispensable role for anti-interference ability by Al–O coordination bond, hydrogen bond, or hydrophobic interactions. Grafted-IIP has good regenerative ability and can be repeated at least six times to treat actual wastewater. The proposed grafted-IIP has wide application prospects for the treatment of the complicated wastewater.

Acknowledgements

This study was financially supported by the National Science Fund for Excellent Young Scholars (51422807), the Natural Science Foundation of China (51238002, 51678285), the Key Project of Science and Technology Department of Jiangxi Province (20143ACG70006) and the Cultivating Project for Academic and Technical Leader of Key Discipline of Jiangxi Province (20153BCB22005).

References

1 N. U. Amin, A. Hussain, S. Alamzeb and S. Begum, Accumulation of heavy metals in edible parts of vegetables irrigated with waste water and their daily intake to adults and children, District Mardan, Pakistan, *Food Chem.*, 2013, **136**(3–4), 1515–1523.
2 M. Arora, B. Kiran, S. Rani, A. Rani, B. Kaur and N. Mittal, Heavy metal accumulation in vegetables irrigated with water from different sources, *Food Chem.*, 2008, **111**(4), 811–815.
3 M. Nakada, K. Fukaya, S. Takeshita and Y. Wada, The accumulation of heavy metals in the submerged plant (Elodea nuttallii), *Bull. Environ. Contam. Toxicol.*, 1979, **22**(1), 21–27.
4 D. C. Bellinger and A. M. Bellinger, Childhood lead poisoning: the torturous path from science to policy, *J. Clin. Invest.*, 2006, **116**(4), 853–857.
5 F. Fu and Q. Wang, Removal of heavy metal ions from wastewaters: a review, *J. Environ. Manage.*, 2011, **92**(3), 407–418.
6 H. A. Naser, Assessment and management of heavy metal pollution in the marine environment of the Arabian Gulf: a review, *Mar. Pollut. Bull.*, 2013, **72**(1), 6–13.
7 A. Nzihou and B. Stanmore, The fate of heavy metals during combustion and gasification of contaminated biomass-a brief review, *J. Hazard. Mater.*, 2013, **256–257**, 56–66.

8 I. R. Pala and S. L. Brock, ZnS nanoparticle gels for remediation of Pb^{2+} and Hg^{2+} polluted water, *ACS Appl. Mater. Interfaces*, 2012, **4**(4), 2160–2167.

9 K. R. Reddy, K. Nakata, T. Ochiai, T. Murakami, D. A. Tryk and A. Fujishima, Nanofibrous TiO_2-Core/Conjugated Polymer-Sheath Composites: Synthesis, Structural Properties and Photocatalytic Activity, *J. Nanosci. Nanotechnol.*, 2010, **10**(12), 7951–7957.

10 K. R. Reddy, K. V. Karthik, S. B. B. Prasad, S. K. Soni, H. M. Jeong and A. V. Raghu, Enhanced photocatalytic activity of nanostructured titanium dioxide/polyaniline hybrid photocatalysts, *Polyhedron*, 2016, **120**, 169–174.

11 K. R. Reddy, M. Hassan and V. G. Gomes, Hybrid nanostructures based on titanium dioxide for enhanced photocatalysis, *Appl. Catal., A*, 2015, **489**, 1–16.

12 B. L. Martins, C. C. V. Cruz, A. S. Luna and C. A. Henriques, Sorption and desorption of Pb^{2+} ions by dead *Sargassum* sp. biomass, *Biochem. Eng. J.*, 2006, **27**(3), 310–314.

13 G. Zhou, J. Luo, C. Liu, L. Chu, J. Ma, Y. Tang, Z. Zeng and S. Luo, A highly efficient polyampholyte hydrogel sorbent based fixed-bed process for heavy metal removal in actual industrial effluent, *Water Res.*, 2016, **89**, 151–160.

14 B. M. W. P. K. Amarasinghe and R. A. Williams, Tea waste as a low cost adsorbent for the removal of Cu and Pb from wastewater, *Chem. Eng. J.*, 2007, **132**(1–3), 299–309.

15 M. K. Mondal, Removal of Pb(II) ions from aqueous solution using activated tea waste: Adsorption on a fixed-bed column, *J. Environ. Manage.*, 2009, **90**(11), 3266–3271.

16 S. Wan, Z. Ma, Y. Xue, M. Ma, S. Xu, L. Qian and Q. Zhang, Sorption of Lead(II), Cadmium(II), and Copper(II) Ions from Aqueous Solutions Using Tea Waste, *Ind. Eng. Chem. Res.*, 2014, **53**(9), 3629–3635.

17 H. Chen, J. Zhao, G. Dai, J. Wu and H. Yan, Adsorption characteristics of Pb(II) from aqueous solution onto a natural biosorbent, fallen Cinnamomum camphora leaves, *Desalination*, 2010, **262**(1–3), 174–182.

18 J. C. Vaghetti, E. C. Lima, B. Royer, B. M. da Cunha, N. F. Cardoso, J. L. Brasil and S. L. Dias, Pecan nutshell as biosorbent to remove Cu(II), Mn(II) and Pb(II) from aqueous solutions, *J. Hazard. Mater.*, 2009, **162**(1), 270–280.

19 S. Wang, Y. Dong, M. He, L. Chen and X. Yu, Characterization of GMZ bentonite and its application in the adsorption of Pb(II) from aqueous solutions, *Appl. Clay Sci.*, 2009, **43**(2), 164–171.

20 G. Yuvaraja, N. Krishnaiah, M. V. Subbaiah and A. Krishnaiah, Biosorption of Pb(II) from aqueous solution by Solanum melongena leaf powder as a low-cost biosorbent prepared from agricultural waste, *Colloids Surf., B*, 2014, **114**, 75–81.

21 M. Hamidpour, M. Kalbasi, M. Afyuni, H. Shariatmadari, P. E. Holm and H. C. Hansen, Sorption hysteresis of Cd(II) and Pb(II) on natural zeolite and bentonite, *J. Hazard. Mater.*, 2010, **181**(1–3), 686–691.

22 Y. Tan, M. Chen and Y. Hao, High efficient removal of Pb(II) by amino-functionalized Fe_3O_4 magnetic nano-particles, *Chem. Eng. J.*, 2012, **191**, 104–111.

23 N. N. Nassar, Rapid removal and recovery of Pb(II) from wastewater by magnetic nanoadsorbents, *J. Hazard. Mater.*, 2010, **184**(1–3), 538–546.

24 L. Yuan and Y. Liu, Removal of Pb(II) and Zn(II) from aqueous solution by ceramisite prepared by sintering bentonite, iron powder and activated carbon, *Chem. Eng. J.*, 2013, **215–216**, 432–439.

25 C. K. Singh, J. N. Sahu, K. K. Mahalik, C. R. Mohanty, B. R. Mohan and B. C. Meikap, Studies on the removal of Pb(II) from wastewater by activated carbon developed from Tamarind wood activated with sulphuric acid, *J. Hazard. Mater.*, 2008, **153**(1–2), 221–228.

26 X. Luo, L. Ding and J. Luo, Adsorptive Removal of Pb(II) Ions from Aqueous Samples with Amino-Functionalization of Metal–Organic Frameworks MIL-101(Cr), *J. Chem. Eng. Data*, 2015, **60**(6), 1732–1743.

27 X. M. Lin, T. T. Li, L. F. Chen, L. Zhang and C. Y. Su, Two ligand-functionalized Pb(II) metal–organic frameworks: structures and catalytic performances, *Dalton Trans.*, 2012, **41**(34), 10422–10429.

28 A. M. Showkat, Y.-P. Zhang, M. S. Kim, A. I. Gopalan, K. R. Reddy and K.-P. Lee, Analysis of Heavy Metal Toxic Ions by Adsorption onto Amino-functionalized Ordered Mesoporous Silica, *Bull. Korean Chem. Soc.*, 2007, **28**(11), 1985–1992.

29 B. Guo, F. Deng, Y. Zhao, X. Luo, S. Luo and C. Au, Magnetic ion-imprinted and –SH functionalized polymer for selective removal of Pb(II) from aqueous samples, *Appl. Surf. Sci.*, 2014, **292**, 438–446.

30 X. Luo, L. Liu, F. Deng and S. Luo, Novel ion-imprinted polymer using crown ether as a functional monomer for selective removal of Pb(II) ions in real environmental water samples, *J. Mater. Chem. A*, 2013, **1**(28), 8280.

31 Y. Zhan, X. Luo, S. Nie, Y. Huang, X. Tu and S. Luo, Selective Separation of Cu(II) from Aqueous Solution with a Novel Cu(II) Surface Magnetic Ion-Imprinted Polymer, *Ind. Eng. Chem. Res.*, 2011, **50**(10), 6355–6361.

32 X. Luo, B. Guo, J. Luo, F. Deng, S. Zhang, S. Luo and J. Crittenden, Recovery of Lithium from Wastewater Using Development of Li Ion-Imprinted Polymers, *ACS Sustainable Chem. Eng.*, 2015, **3**(3), 460–467.

33 X. Cai, J. Li, Z. Zhang, F. Yang, R. Dong and L. Chen, Novel Pb^{2+} ion imprinted polymers based on ionic interaction *via* synergy of dual functional monomers for selective solid-phase extraction of Pb^{2+} in water samples, *ACS Appl. Mater. Interfaces*, 2014, **6**(1), 305–313.

34 P. A. B. da Silva, G. C. S. de Souza, D. M. d. S. Leotério, M. F. Belian, W. E. Silva, A. P. S. Paim and A. F. Lavorante, Synthesis and characterization of functionalized silica with 3,6-ditia-1,8-octanediol for the preconcentration and determination of lead in milk employing multicommuted flow system coupled to FAAS, *J. Food Compos. Anal.*, 2015, **40**, 177–184.

35 X. Luo, W. Zhong, J. Luo, L. Yang, J. Long, B. Guo and S. Luo, Lithium ion-imprinted polymers with hydrophilic PHEMA polymer brushes: The role of grafting density in anti-

interference and anti-blockage in wastewater, *J. Colloid Interface Sci.*, 2017, **492**, 146–156.

36 M. Zhao, X. Chen, H. Zhang, H. Yan and H. Zhang, Well-defined hydrophilic molecularly imprinted polymer microspheres for efficient molecular recognition in real biological samples by facile RAFT coupling chemistry, *Biomacromolecules*, 2014, **15**(5), 1663–1675.

37 G. Pan, Y. Ma, Y. Zhang, X. Guo, C. Li and H. Zhang, Controlled synthesis of water-compatible molecularly imprinted polymer microspheres with ultrathin hydrophilic polymer shells *via* surface-initiated reversible addition–fragmentation chain transfer polymerization, *Soft Matter*, 2011, **7**(18), 8428.

38 X. Luo, Y. Xi, H. Yu, X. Yin and S. Luo, Capturing Cadmium(II) Ion from Wastewater Containing Solid Particles and Floccules Using Ion-Imprinted Polymers with Broom Effect, *Ind. Eng. Chem. Res.*, 2017, **56**(9), 2350–2358.

39 Y. Ma, G. Pan, Y. Zhang, X. Guo and H. Zhang, Narrowly dispersed hydrophilic molecularly imprinted polymer nanoparticles for efficient molecular recognition in real aqueous samples including river water, milk, and bovine serum, *Angew. Chem., Int. Ed.*, 2013, **52**(5), 1511–1514.

40 Y. Ma, Y. Zhang, M. Zhao, X. Guo and H. Zhang, Efficient synthesis of narrowly dispersed molecularly imprinted polymer microspheres with multiple stimuli-responsive template binding properties in aqueous media, *Chem. Commun.*, 2012, **48**(50), 6217–6219.

41 M. U. Khan, K. R. Reddy, T. Snguanwongchai, E. Haque and V. G. Gomes, Polymer brush synthesis on surface modified carbon nanotubes *via in situ* emulsion polymerization, *Colloid Polym. Sci.*, 2016, **294**(10), 1599–1610.

42 M. Hassan, K. R. Reddy, E. Haque, A. I. Minett and V. G. Gomes, High-yield aqueous phase exfoliation of graphene for facile nanocomposite synthesis *via* emulsion polymerization, *J. Colloid Interface Sci.*, 2013, **410**, 43–51.

43 H. Liu, F. Yang, Y. Zheng, J. Kang, J. Qu and J. P. Chen, Improvement of metal adsorption onto chitosan/*Sargassum* sp. composite sorbent by an innovative ion-imprint technology, *Water Res.*, 2011, **45**(1), 145–154.

44 G. X. Yang and H. Jiang, Amino modification of biochar for enhanced adsorption of copper ions from synthetic wastewater, *Water Res.*, 2014, **48**, 396–405.

45 H. Hintz, H. Peisert, H. J. Egelhaaf and T. Chassé, Reversible and Irreversible Light-Induced p-Doping of P3HT by Oxygen Studied by Photoelectron Spectroscopy (XPS/UPS), *J. Phys. Chem. C*, 2011, **115**(27), 13373–13376.